Pinning and depinning of two quantized vortices in superfluid ^{4}He

Makoto Tsubota and Susumu Maekawa
Institute of Fluid Science, Tohoku University, Sendai 980, Japan
(Received 7 December 1992)

Three-dimensional dynamics of two interactive quantized vortices trapped by a pinning site is studied. This paper discusses their pinning and depinning mechanisms, and the effect of an applied superflow field. The equations of motion and the method of numerical calculation follow Schwarz. Assume that there is a vortex near a pinning site that has already captured another. Then we have generally two cases; vorticity of the new vortex is antiparallel or parallel to that of the original one. These two cases are shown to go through different processes. An antiparallel vortex is attracted into the pinning site to reconnect with the original vortex. The resulting vortices leave there because of their self-induced motion, none being left behind. On the other hand, a parallel vortex can reach the pinning site only when the initial position and the applied field satisfy some condition, because the interaction between two vortices tends to prevent the new vortex from approaching. Two parallel vortices once trapped by the pinning site relax to a stationary configuration because of mutual friction. The critical depinning superflow velocity for two parallel vortices is smaller than that for only one. The obtained results are compared with some experimental works.

I. INTRODUCTION

Superfluid ^{4}He (Helium II) behaves like an irrotational ideal fluid, whose characteristic phenomena can be explained well by the Landau two-fluid model. However, superflow becomes dissipative (superfluid turbulence) above some critical velocity. The transition to the dissipative flow is generally thought to be closely connected with the quantized vortex[1] characterized by quantization of its circulation and the very thin core radius of the order of atomic size. Because of the latter property, quantized vortices are easily pinned even by a local protrusion of a few angstroms, so that vortex pinning is expected to occur always in usual superflow.

These pinning and depinning processes of vortices have played an important role in various interesting phenomena in superfluid ^{4}He. Hegde and Glaberson performed a series of experiments in order to study the effect of surface roughening on the onset of vortex motion in thermal counterflow in a rotating channel.[2] Rough surfaced channels exhibit a larger observed critical velocity than smooth ones, which suggests that static pinning is important. Adams *et al.* investigated experimentally the spin-up problem and observed the recovery of the solid-body rotation of the liquid.[3] The transient phenomenon was found to depend on surface roughening of the disk cell. The problem of remnant vortices is also important. This is related to a mystery of how vortices sustaining turbulence are initially generated. Experiments by Awschalom and Schwarz show that a superfluid at rest contains a substantial number of residual pinned vortices generated upon cooling through the λ transition.[4]

The issue of vortex pinning may also be concerned with the recent experiments on phase slippage. Investigating superflow oscillating through a small orifice, Avenel and Varoquaux found that a discrete amount of energy is suddenly dissipated whenever the flow velocity exceeds a critical value.[5] Amar *et al.* studied phase slippage in an apparatus of a simpler topology to that of Avenel and Varoquaux, and pointed out that the phenomena depend a great deal on the orifice geometry.[6] One of the important problems is whether such a phenomenon can be understood within a hydrodynamical context or only by some new quantum-mechanical mechanism, such as the quantum-mechanical nucleation of quantized vortices. Davis *et al.*[7] and Ihas *et al.*[8] found the transition from thermal to quantum nucleation of vortices below a crossover temperature of 200 and 147 mK, respectively.

Schwarz has developed successfully a numerical analysis of three-dimensional dynamics of quantized vortices and gave an excellent picture of the self-sustaining vortex tangle state for superfluid turbulence.[9,10] He also made a numerical calculation of vortex pinning. The important feature of the calculation was using no phenomenological parameters. The calculated critical depinning superflow and normal flow velocity of a vortex trapped by a pinning site agreed well with his analytical criterion, which will be described in Sec. III. About the above phase slippage, Schwarz showed numerically that microscopic surface roughness can lead to a dissipative vortex motion and vortex regeneration,[11] and the dependence of the critical velocity on temperature results from a thermal fluctuation of pinned vortices.[12] It was also shown that under superflow the above remnant pinned vortices act as a continuous source of vortices to sustain the vortex tangle in turbulence.[13]

The above works are concerned with pinning of one vortex. No usual surfaces are specular for a vortex with such a thin core. If vortices are dense on the surface, two vortices may happen to be trapped together by a pinning site. Then, since the interaction between two vortices works, the dynamics can be much different from that of

only one trapped on a pinning site. Previously we investigated numerically the interactive motion of two close vortices, which was shown to depend a great deal on the relative direction of their vorticities.[14] About antiparallel vortices approach each other making small cusps on their nearest parts to reconnect eventually, while about parallel ones do a rotational motion around each other to dodge. These results can also be applicable to two vortices captured by a pinning site.

Thus this paper describes the dynamics of two interactive vortices trapped on a pinning site. The equations of motion of vortices and the method of numerical calculation are briefly described in Sec. II. Section III refers to depinning of one vortex trapped by a pinning site. Our first problem is whether one vortex can be attracted by a pinning site that has already captured another; it is discussed in Sec. IV. Since the answer is positive, the second problem is the interactive motion of two vortices on a pinning site and the effect of an applied flow field, which is described in Sec. V. Section VI summarizes the complicated story of two vortices on a pinning site. Throughout this work we have two cases; two vortices are parallel or antiparallel. These two cases are shown to go through different processes.

II. MOTION OF A VORTEX AND NUMERICAL CALCULATION

This section describes briefly the basic equations of motion[1] and the method of numerical calculation. A vortex filament is defined by a thin core passing through the fluid and has a definite direction which shows the vorticity. Except for the core region, the superflow velocity field has a classically well-defined meaning and can be described by ideal fluid dynamics. The velocity produced at a point $\mathbf{r}$ by a vortex filament is given by the Biot-Savart expression:

$$\mathbf{v}_{s,\omega}(\mathbf{r},t)=\frac{\kappa}{4\pi}\int_L \frac{(\mathbf{s}_1-\mathbf{r})\times d\mathbf{s}_1}{|\,\mathbf{s}_1-\mathbf{r}\,|^3}, \tag{1}$$

where κ is the quantized value of circulation. The filament is represented by the parametric form $\mathbf{s}=\mathbf{s}(\xi,t)$, $\mathbf{s}_1$ refers to a point on the filament and the integration is taken along the filament. Since the inertia of the core is neglected, an element on the filament always moves with the superflow velocity at the point in the absence of dissipation. Attempting to calculate the velocity at a point $\mathbf{r}=\mathbf{s}$ on the filament makes the integral diverge as $\mathbf{s}_1\to\mathbf{s}$. To avoid it, we follow Schwarz's method;[9] the propagation velocity $\dot{\mathbf{s}}$ of the vortex filament at point $\mathbf{s}$ is divided into two components:

$$\dot{\mathbf{s}}=\frac{\kappa}{4\pi}\mathbf{s}'\times\mathbf{s}''\ln\left(\frac{2(l_+l_-)^{1/2}}{e^{1/4}a_0}\right)+\frac{\kappa}{4\pi}\int_L{}' \frac{(\mathbf{s}_1-\mathbf{s})\times d\mathbf{s}_1}{|\,\mathbf{s}_1-\mathbf{s}\,|^3}. \tag{2}$$

The first term indicates the local-induced field arising from a curved line element acting on itself, where l_+ and l_- are the lengths of the two adjacent line elements that hold the point $\mathbf{s}$ between, and the prime denotes differentiation with respect to the arc length ξ. The second term represents the nonlocal field obtained by carrying out the integral of Eq. (1) along the rest of the filament and any other filaments that may be present.

If boundaries are present, a velocity field $\mathbf{v}_{s,b}$ is added to $\mathbf{v}_{s,\omega}$. This boundary-induced field satisfies $\nabla\cdot\mathbf{v}_{s,b}=0$, $\nabla\times\mathbf{v}_{s,b}=\mathbf{0}$ subject to the boundary condition:

$$(\mathbf{v}_{s,b}+\mathbf{v}_{s,\omega})\cdot\hat{\mathbf{n}}=0. \tag{3}$$

When boundaries are specular plane surfaces, $\mathbf{v}_{s,b}$ is just the field by an image vortex made by reflecting the filament into the plane and reversing its direction of vorticity. When there is a hemispherical pinning site on a flat surface, another field $\mathbf{v}_{s,p}$ must be added to $\mathbf{v}_{s,b}$ so that the above boundary condition is satisfied. The analytical velocity potential arising from the line element $d\mathbf{s}_1$ is

$$d\Phi_{b,\mathrm{out}}=\frac{\kappa}{4\pi}\,ds_\perp\,\frac{b\sin\phi}{s_1 r}\sum_{n=1}^{\infty}\left[\frac{b^2}{s_1 r}\right]^n\frac{P_n^1(\cos\theta)}{n+1} \tag{4}$$

when the element is outside the sphere, and

$$d\Phi_{b,\mathrm{in}}=\frac{\kappa}{4\pi}\,ds_\perp\,\frac{\sin\phi}{r}\sum_{n=1}^{\infty}\left[\frac{s_1}{r}\right]^n\frac{P_n^1(\cos\theta)}{n+1} \tag{5}$$

when it is inside the sphere.[9] Here, P_n^1 are the associated Legendre polynomials, b is the sphere radius, and the used spherical coordinate system is shown in Fig. 1. Summing $d\Phi$ over the entire vortice yields the total potential due to the pinning site. Then we have to change the spherical coordinate system from one line element to another. Some other applied field $\mathbf{v}_{s,a}$, if present, must be added, which results in the total velocity $\dot{\mathbf{s}}_0$ of the vortex filament without dissipation:

$$\dot{\mathbf{s}}_0=\frac{\kappa}{4\pi}\,\mathbf{s}'\times\mathbf{s}''\ln\left(\frac{2(l_+l_-)^{1/2}}{e^{1/4}a_0}\right)+\frac{\kappa}{4\pi}\int_L{}' \frac{(\mathbf{s}_1-\mathbf{s})\times d\mathbf{s}_1}{|\,\mathbf{s}_1-\mathbf{s}\,|^3}+\mathbf{v}_{s,b}(\mathbf{s})+\mathbf{v}_{s,a}(\mathbf{s}). \tag{6}$$

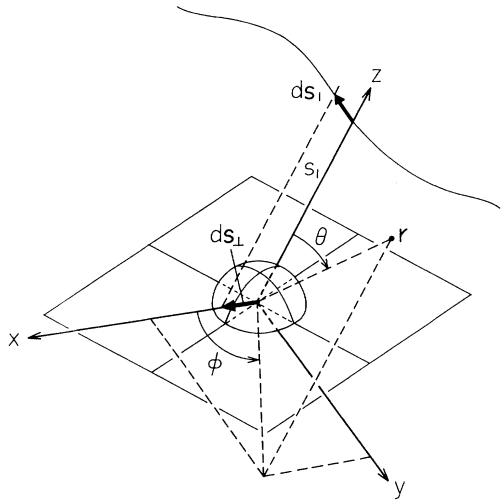

FIG. 1. Coordinate system used for calculating $\mathbf{v}_{s,p}$.

Mutual friction that is characteristic in He II must be taken into account. Then the velocity of a point $\mathbf{s}$ on a vortex filament is given by

$$\dot{\mathbf{s}} = \dot{\mathbf{s}}_0 + \alpha \mathbf{s}' \times (\mathbf{v}_n - \dot{\mathbf{s}}_0) - \alpha' \mathbf{s}' \times [\mathbf{s}' \times (\mathbf{v}_n - \dot{\mathbf{s}}_0)], \quad (7)$$

where α and α' are the temperature-dependent friction coefficients, and $\dot{\mathbf{s}}_0$ is calculated from Eq. (6). We take $\alpha = 0.1$ and $\alpha' = 0$ for simplicity throughout this work.

All calculations in this work have been done for a superfluid confined between two smooth plates spaced a distance D apart, one of which contains a pinning site. We used the particular values $D = 10^{-3}$ cm and $b = 10^{-4}$ cm. Although the dependence of obtained results on the values of D and b is important, the main purpose of this paper is to reveal the essence of motion before everything.

This work is confined to a pure superflow. An investigation of the effect of normal flow, whose importance to vortex dynamics is pointed out,[9,15] will be reported elsewhere.

We follow Schwarz in the methods of numerical calculations.[9] A vortex filament is represented by a single string of points. The vortice configuration of the moment determines the velocity field in the fluid, thus moving the points on vortex filaments by Eqs. (6) and (7). Both local and nonlocal terms are represented by means of line elements connecting two adjacent points. As discussed in Ref. 9, the explicit forward integration of the local term can be numerically unstable. To prevent this difficulty, a modified hopscotch algorithm is adopted. As the vortex configuration develops and, particularly, two vortices approach each other, the length of a line element can increase or decrease. Then it is necessary to add or remove points properly so that the local resolution does not lose.

III. CRITICAL DEPINNING VELOCITY OF ONE VORTEX

Previous to the depinning problem of two vortices, this section describes that of one vortex; this is neccesary for the following sections. The motion of a vortex attracted into a pinning site was studied in detail by Schwarz.[9] The characteristic case he studies is a straight vortex extending between two smooth planes, one of which contains the pinning site. The boundary field tries to move the line around the sphere. The closer a line element is to the sphere, the stronger the field acting on it becomes, which distorts the vortex. The resulting self-induced field and mutual friction cause the vortex to spiral into the sphere. When the vortex gets close enough, a cusp is pulled out. Then Schwarz follows the plausible, but a little artificial, procedure; as the vortex approaches the pinning site infinitely closely, there occurs a kind of reconnection that pulls up the closest end point of the vortex onto the sphere surface. Afterwards the vortex climbs up on the sphere spiraling in, thus standing up eventually on the top. We have confirmed numerically this process except for the reconnection.

An applied superflow field modifies the above motion. Since the applied field intends to wash away the vortex, it can be captured by the pinning site only when it passes by the site within a critical distance that depends on the sphere size and the amplitude of the field. Furthermore, the trapped vortex is also influenced by the applied field. The eventual equilibrium configuration of the vortex is determined by the balance between the applied field and the self-induced one resulting from the distortion; the vortex stands up against the applied field by bending like a bow. The curvature of the vortex increases with the applied field. Finally the vortex cannot get such a stationary configuration for large applied fields, thus becoming depinned from the site. Considering this mechanism, Glaberson and Donnelly gave a critical depinning velocity

$$\mathbf{v}_{s,\mathrm{pin}} = \frac{\kappa}{2\pi D} \ln\left[\frac{4D}{e^{1/4} a_0}\right], \quad (8)$$

where D is a characteristic dimension across the channel.[16] The dependence of D on the critical velocity is consistent with experimental results.

The representation includes no parameters of the pinning site. Schwarz analyzed the equilibrium shape of the vortex in more detail and obtained the critical velocity with the radius b of the sphere;[9]

$$\mathbf{v}_{s,\mathrm{pin}} = \frac{\kappa}{2\pi D} \ln\left[\frac{b}{a_0}\right]. \quad (9)$$

He also made the numerical calculation of one-vortex depinning, whose results agreed quantitatively with the equation.

We investigated numerically this problem too. An initial configuration of a vortex captured by a pinning site is allowed to evolve under the influence of an applied superflow field. Following the motion to the stationary state judges whether the vortex is depinned from the sphere or stays there to find the critical depinning velocity. However, the obtained critical velocity $v_{p,1}$ differs a little from one initial configuration to another.

A few typical examples are shown in Fig. 2. A vortex, whose self-induced field is initially parallel to the applied one, is blown down once [Fig. 2(a)]. It recovers, however, before depinning, thus getting finally to the stationary configuration where the applied field blows against the self-induced one. On the other hand, when the self-induced field is initially almost antiparallel to the applied one, the vortex can easily reach the stationary configuration only by a small distortion [Fig. 2(b)]. The former is the relaxation from large deviation, while the latter is that from small one. As a result, the value of $v_{p,1}$ of the latter is larger than that of the former. This is the reason why the values of critical velocity cover some range. The obtained values shown in Fig. 3 are entirely smaller than those of Schwarz; the reason is not clear.

IV. MOTION OF A VORTEX NEAR THE PINNING SITE WITH ANOTHER VORTEX

This section discusses whether the pinning site that has already captured a vortex (vortex A) can trap another vortex (vortex B). Vortex B is subject not only to the boundary-induced field that tends to rotate it around

the sphere, but to the nonlocal field from vortex A. Then there are two cases corresponding to whether two vortices are parallel or antiparallel. Furthermore their motion is affected by an applied superflow field.

A. Motion of an antiparallel pair

Figure 4(a) shows the motion of an antiparallel pair without an applied field. Vortex A is assumed to stand upright on the top of the sphere initially. Vortex B is found to always be attracted to the sphere. For vortex B, the nonlocal field made by A follows nearly the same direction as the boundary-induced one. Consequently the attraction mechanism described in the last section is still effective, pulling up the end point of B onto the sphere. The pulled-up vortex B never failed to reconnect with A, whose process is described in detail in Sec. V. Another initial configuration of B is also possible as shown in Figs. 4(b) and 4(c). Although vortex B is attracted as a whole, it reconnects with A before getting on the sphere, which leads to two new vortices; one is on the sphere and the other is not. The upper one leaves the site immediately owing to its self-induced field. The motion of the lower one is shown in Fig. 5. The end point on the sphere slips down, the vortex leaving it. It is only these two kinds of reconnection that are allowed topologically. In any case two antiparallel vortices are destined not to be pinned by the pinning site.

The effect of an applied superflow field on their motion is shown in Figs. 6(a)–6(c). It becomes evident that the above two kinds of motion can occur even under an applied field. A too strong field, however, would blow vortex A off from the pinning site or take vortex B away keeping it from the attraction.

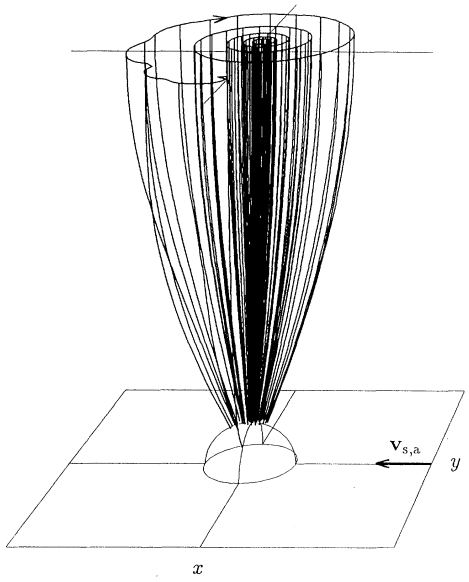

(a)

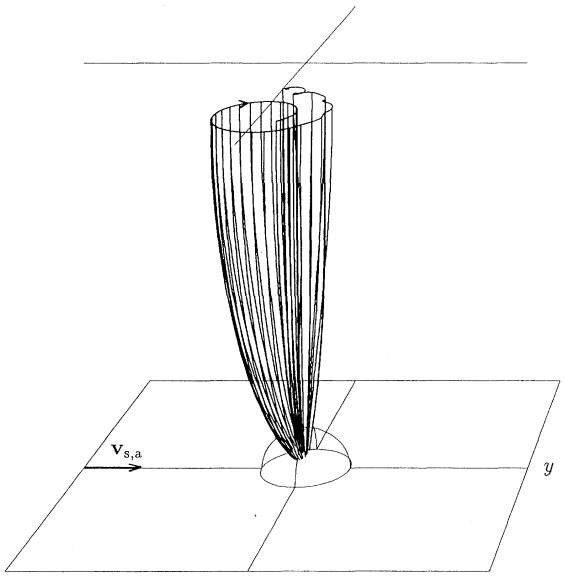

(b)

FIG. 2. Motion of a vortex under an applied superflow field $\mathbf{v}_{s,a}$. The arrow on the top shows the direction of motion: (a) $v_{s,a} = 0.1$ cm/sec, (b) $v_{s,a} = 0.4$ cm/sec.

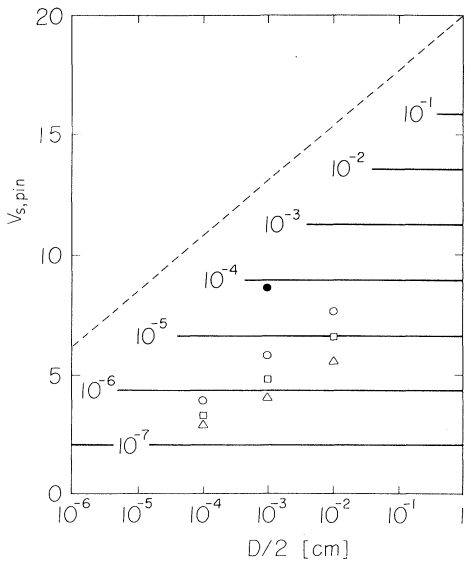

FIG. 3. Critical depinning velocity of one vortex in units of $\kappa/2\pi D$. The solid lines refer to Eq. (9) for various values of b in cm. The dashed line refers to Eq. (8). The obtained values for $(D/2, b) = (10^{-4}, 10^{-5})$, $(10^{-3}, 10^{-4})$, and $(10^{-2}, 10^{-3})$ are shown. The open circles and the triangles correspond to the initial configurations antiparallel and parallel, respectively, to the applied field; both lower parts make an angle of 45° with the z axis. The squares means the initial configuration where the vortex stands up on the top of the sphere. The filled circle shows the value for $D/2 = 10^{-3}$ cm and $b = 10^{-4}$ cm calculated by Schwarz (Ref. 9).

B. Motion of a parallel pair

The motion of a parallel pair is more complicated. Then, for vortex B, the nonlocal field from A and the boundary-induced one tend to cancel each other. Their values become comparable in amplitude when the distance d between vortex B and the pinning site center is equal to a critical distance d_c determined by the sphere radius b. If d is smaller than d_c, vortex B is rotated around the sphere by the boundary-induced field superior to the nonlocal one, thus being captured [Fig. 7(a)]. The numerical calculation finds that d_c is about $1.2b$. The values of d larger than d_c cause the nonlocal field to dominate the boundary-induced one. The nonlocal interaction generally tends to rotate two parallel vortices about a point halfway between them. If vortex B happens to be close to the pinning site within d_c during the rotation, it is attracted by the boundary-induced field [Fig. 7(b)]. As long as it does not approach the sphere within d_c, it cannot be captured, because the boundary-induced field does not work [Fig. 7(c)]. In contrast to the attraction by a pinning site with no vortices, the mutual friction makes vortex B spiral out from the sphere. During the rotation of B, vortex A is trapped on the site. This is because the direction of the nonlocal velocity made by B is changing continuously even if the amplitude exceeds that of the critical depinning velocity discussed in the last section.

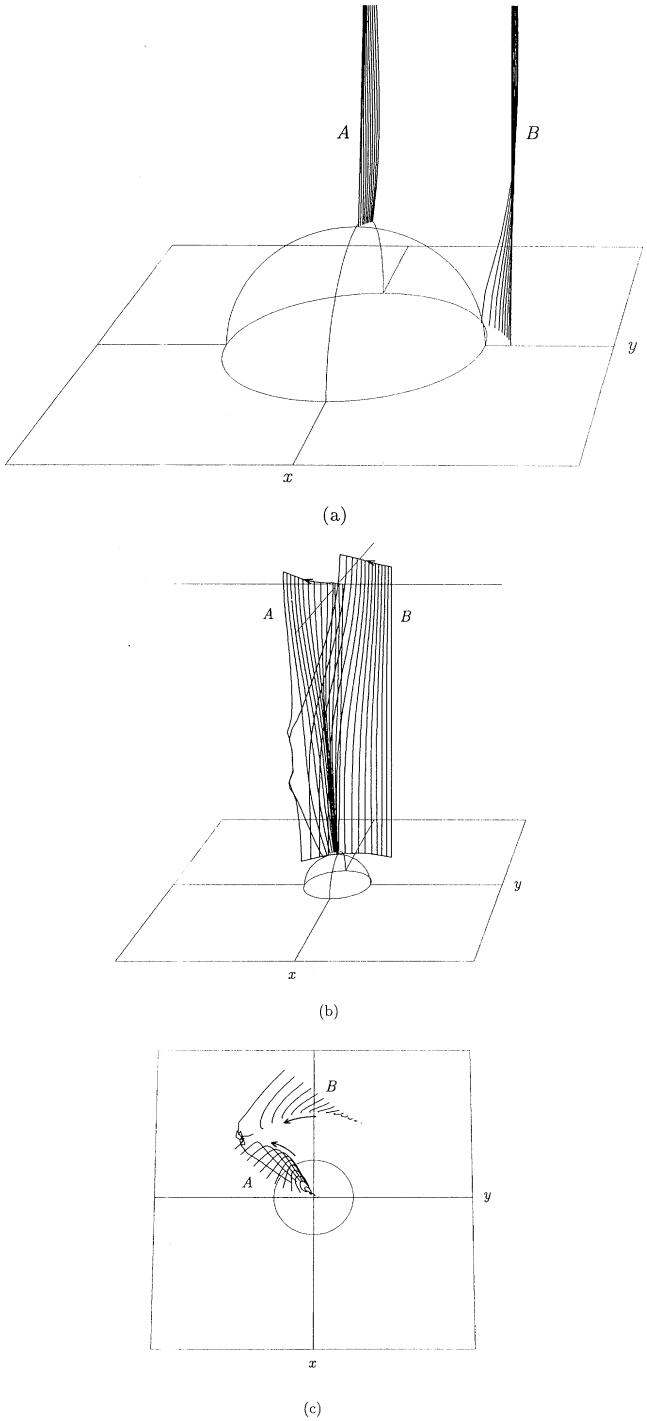

FIG. 4. Motion of an antiparallel pair without an applied field. (c) represents the top view of (b).

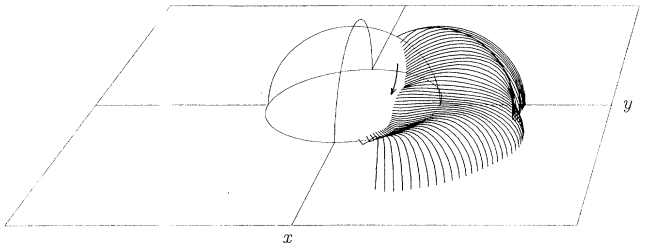

FIG. 5. Motion of the vortex left after the reconnection of two antiparallel vortices.

An applied superflow field has a great effect on the behavior of the parallel pair. Figure 7(d) shows that the applied field moves vortex B to the pinning site getting over the nonlocal interaction. Whether vortex B can reach the sphere depends on the applied field and its initial position relative to the sphere. We followed the motion of vortex B that was initially parallel to the z axis. The initial end point on the x-y plane is given by the coordinates $(-2b, y_i)$. Figure 8 shows the trajectory of the end point on the plane for various initial values of y_i under an applied field of $v_{s,a} = 0.5$ cm/sec. Only vortices within the range from $y_i = 0.5b$ to $y_i = 3b$ can arrive at the sphere. The range increases with the amplitude of $v_{s,a}$. The case of Fig. 8 has a critical velocity v_c below which any vortex B never reaches the site; the value of v_c is found to be about 0.3 cm/sec.

V. MOTION OF TWO VORTICES TRAPPED ON A PINNING SITE

As discussed in the last section, a vortex can be attracted to the pinning site with another under some conditions. This section investigates their motion after both were trapped on the sphere.

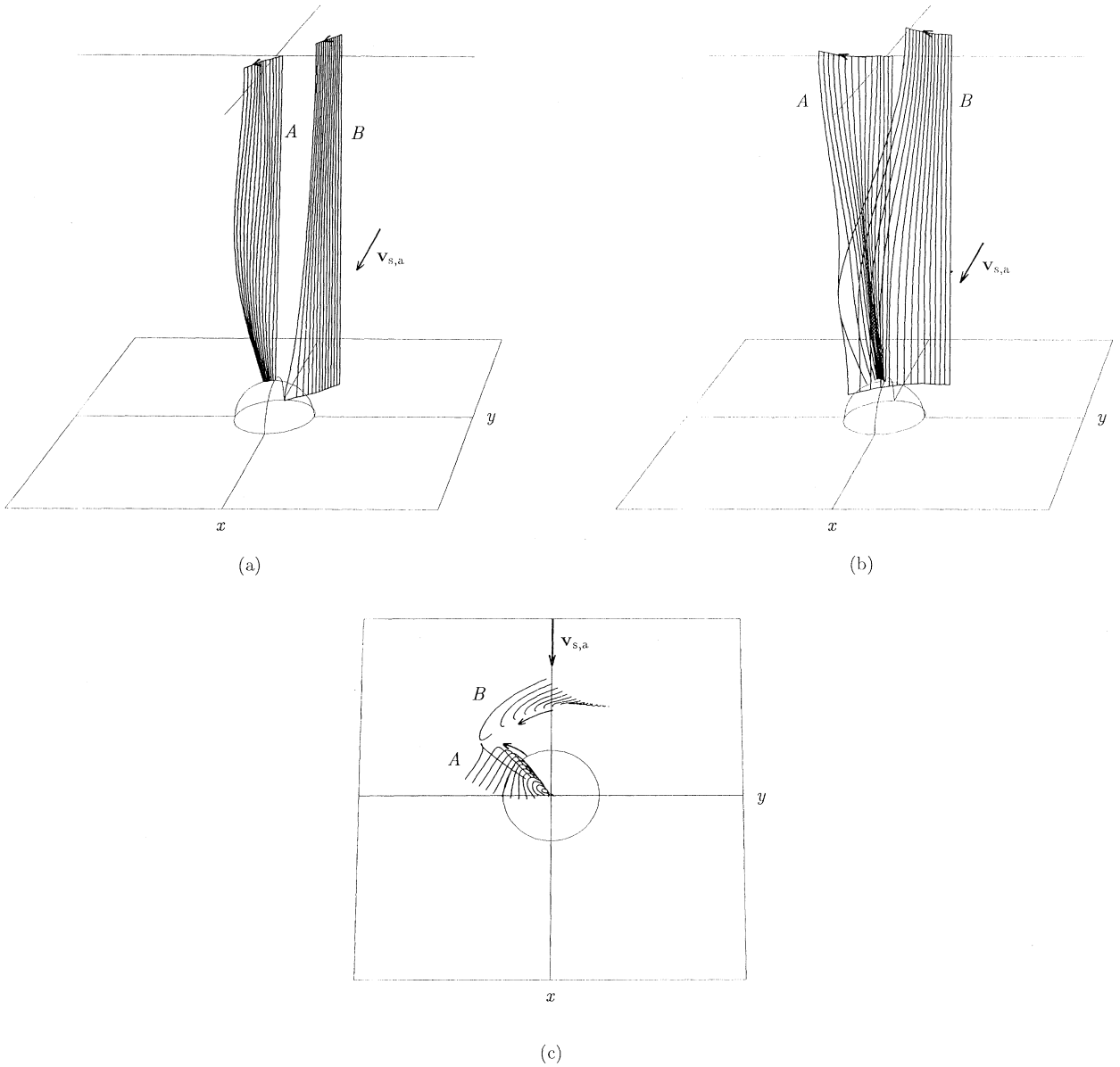

FIG. 6. Motion of an antiparallel pair with an applied field. (c) represents the top view of (b).

A. Motion of an antiparallel pair

Figure 9 shows the typical motion. Both the nonlocal field from the partner and the boundary-induced one have the component directed to the x axis, which moves the vortices. Since the boundary-induced field also tends to rotate them toward the direction opposite to each other, their end points get close on the sphere. Their collision leads to a reconnection of two vortices. The resulting vortex leaves the pinning site because of its self-induced field. It might be due to the initial configuration that these two vortices reconnect just on the sphere. Another kind of reconnection is shown in Fig. 10; this can be regarded as a rather general case. Two vortices reconnect at a point not on the sphere, which produces two new vortices. The upper one leaves the sphere similarly.

The motion of the lower one is shown in Fig. 11. Both end points on the site become close to each other because of the self-induced and boundary-induced fields, which is similar to the situation of Fig. 9. There is, however, a great difference between the present and previous cases. During the approach of both end points, the plane including the vortex is inclining. This reminds us of the motion of a vortex ring moving parallel to a specular surface; the image field acts most strongly on the part nearest the surface, retarding it. In our present case, the image field prevents the end points from moving, thus causing that incline of the vortex. The vortex which has

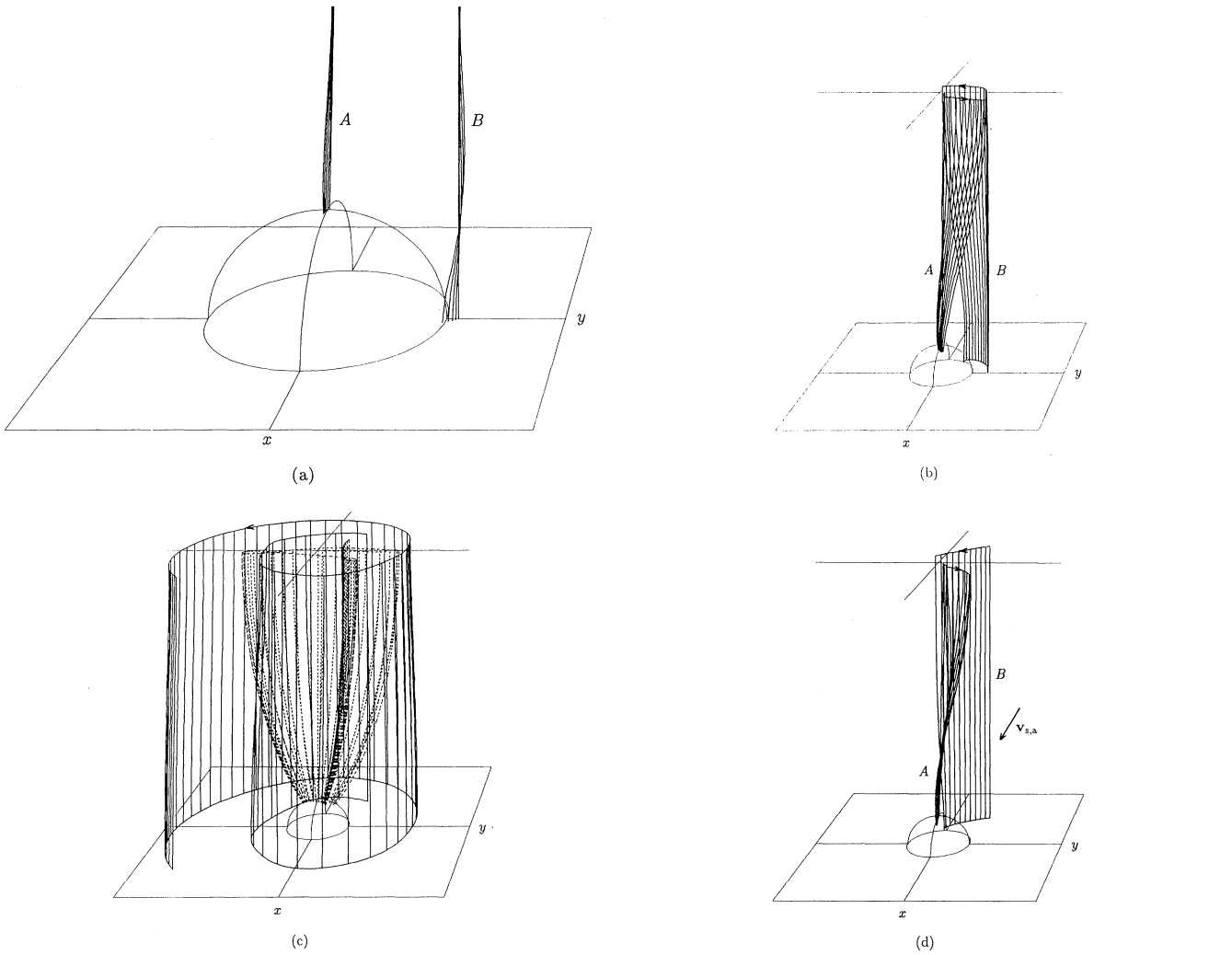

FIG. 7. Motion of a parallel pair: (a), (b), and (c) without an applied field, while (d) with a field. In (c) the dotted and solid lines refer to vortices A and B, respectively.

become almost parallel to the surface begins to proceed toward the surface, expanding under the effect of the image field. Investigating the last destiny of the vortex is beyond hydrodynamics using the Biot-Savart law. It is sure, however, that the vortex gets depinned from the pinning site.

So far, we have seen that two antiparallel vortices pinned on a pinning site make some reconnection or other to get depinned from the site. Advancing very rapidly, the depinning process is influenced little by an applied superflow field so far as it is not so large as to blow them off.

B. Motion of a parallel pair

Two parallel vortices pinned as described in Sec. IV begin to rotate around the pinning site. Figure 12 shows the motion starting from a comparatively symmetrical initial configuration. The rotation direction shows that it results from neither the local nor boundary-induced field,

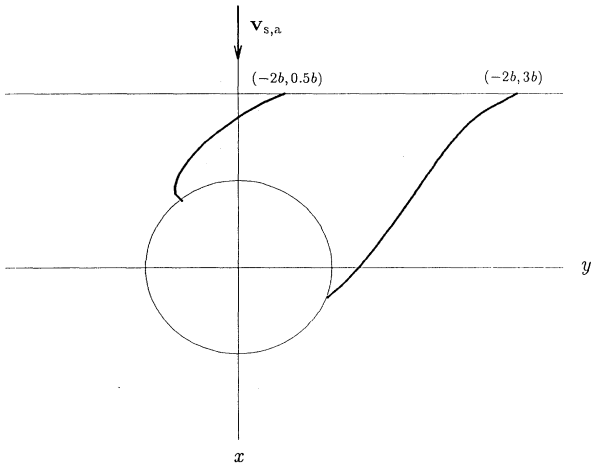

FIG. 8. Trajectory on the x-y plane of vortex B under an applied field $v_{s,a} = 0.5$ cm/sec. The initial end point is given by the coordinates $(-2b, y_i)$. Only vortices starting from the range $0.5b < y_i < 3b$ can reach the pinning site.

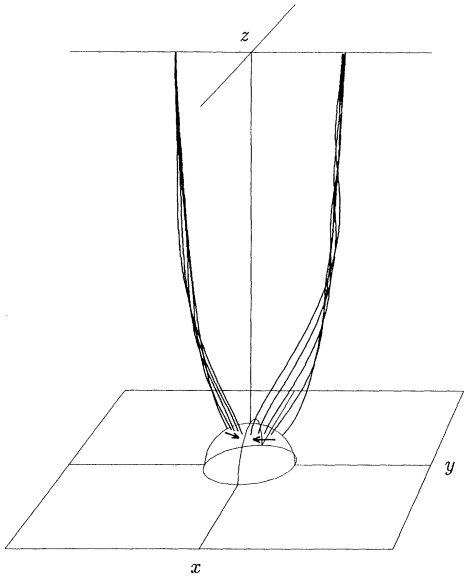

FIG. 9. Motion of an antiparallel pair on a pinning site. The arrows represent the direction of motion.

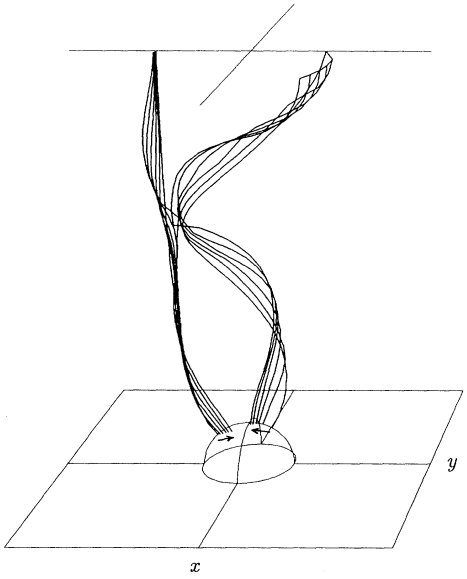

FIG. 10. Another motion of an antiparallel pair.

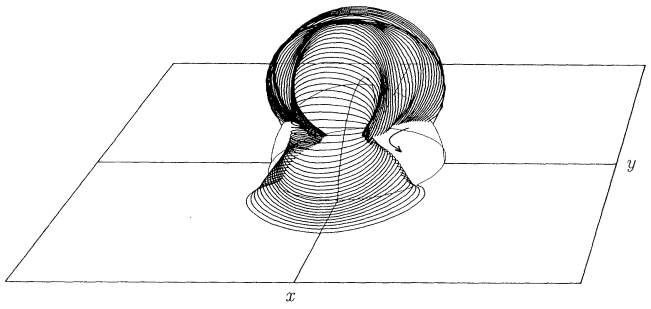

FIG. 11. Motion of the vortex left after the reconnection of two antiparallel vortices on the sphere.

but the nonlocal field between them. The vortices rotate keeping their interval nearly constant. Mutual friction depresses, however, gradually the rotation to lead to a stationary configuration which is balanced between the nonlocal and local fields. It is impossible to obtain the analytical representation of the equilibrium configuration.

Another motion starting from an asymmetrical initial state is shown in Fig. 13. The initial configuration consists of two vortices placed in the x-z and y-z planes whose lower parts make an angle of 30° and 45°, respec-

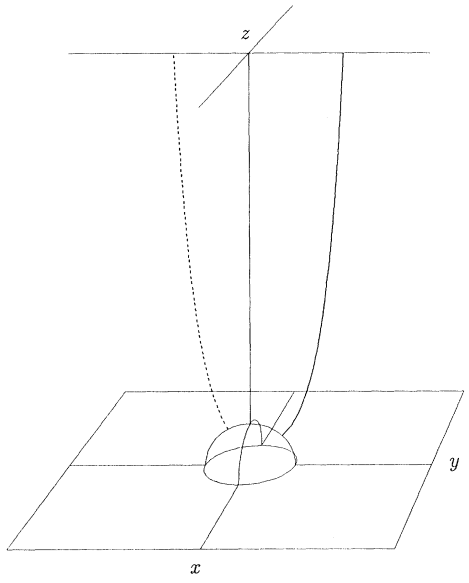

(a)

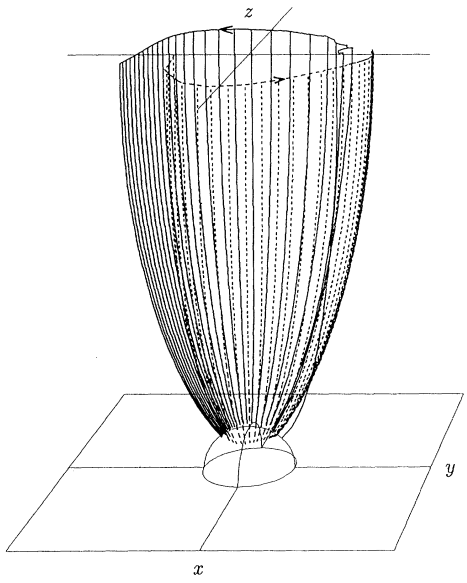

(b)

FIG. 12. Motion of a parallel pair on a pinning site. (a) is the initial configuration. The arrows on the top refer to the direction of motion.

tively, with the z axis. As soon as the motion starts, they arrange themselves so that they are opposite each other, in other words, included in an identical plane. As two vortices rotate around the z axis, their angles made with it oscillate out of phase. Eventually mutual friction relaxes the motion to the symmetrical stationary configuration.

C. Critical depinning velocity of two parallel vortices

The stationary configuration of two parallel vortices described in the last subsection can be influenced more or less by an applied superflow field. A small field would only modify the equilibrium, while a large enough one could distort it so much as to drag the vortices out of the pinning site. This subsection describes the effect of an applied field on the motion of two parallel vortices trapped on the sphere.

The stationary configuration without a field is adopted as the initial condition. Figure 14 shows how a relatively small field changes it, where the field is applied perpendicular to the plane including initially two vortices. The new equilibrium state breaks the symmetry of two vortices. The curvature of vortex A becomes smaller than the original, while that of vortex B increases oppositely. This is because the nonlocal field from the partner, which the local-induced one should cancel, is antiparallel to the

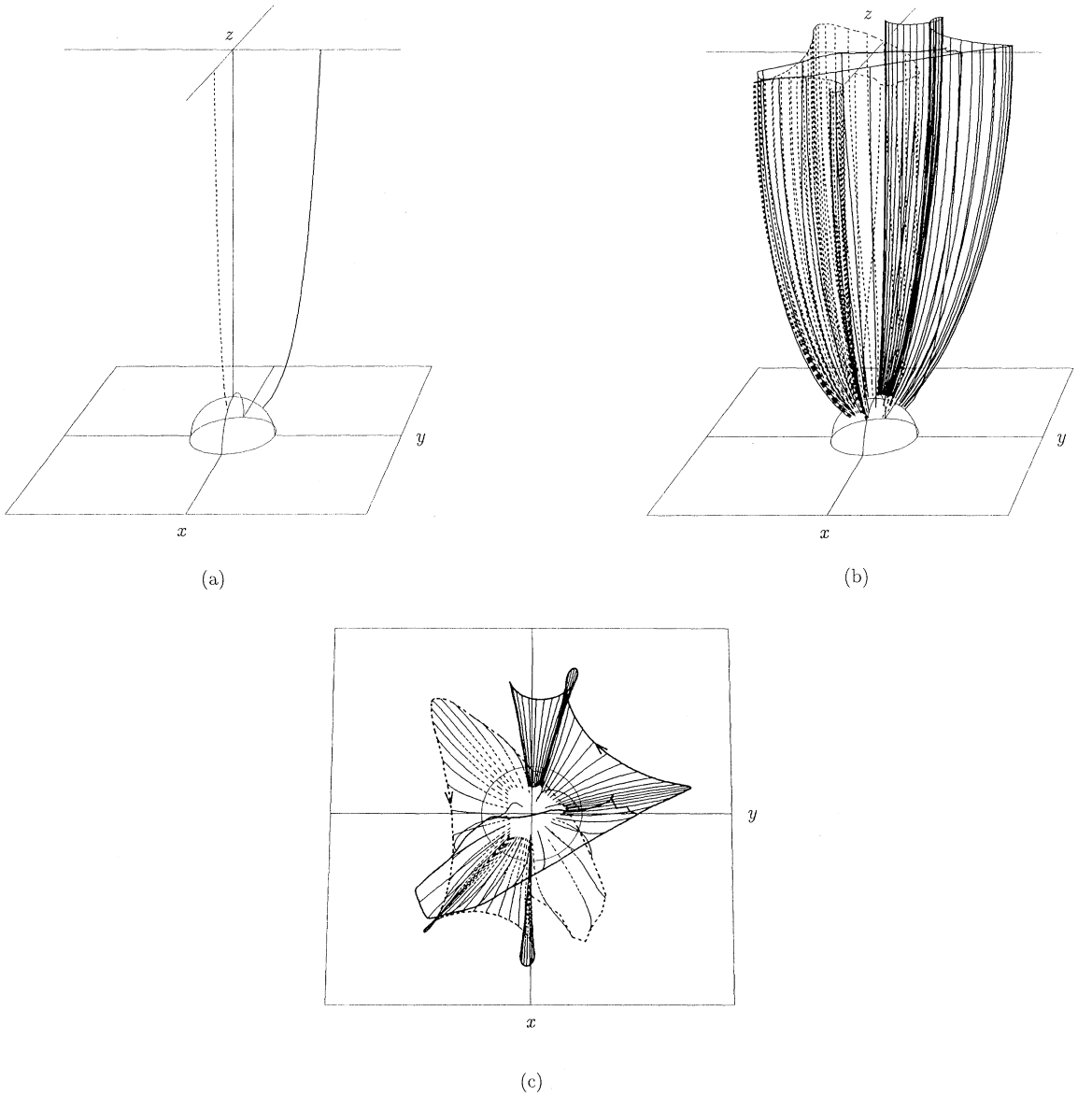

FIG. 13. Another motion of a parallel pair on a pinning site; (c) is the top view of (b). (a) is the initial configurations of two vortices.

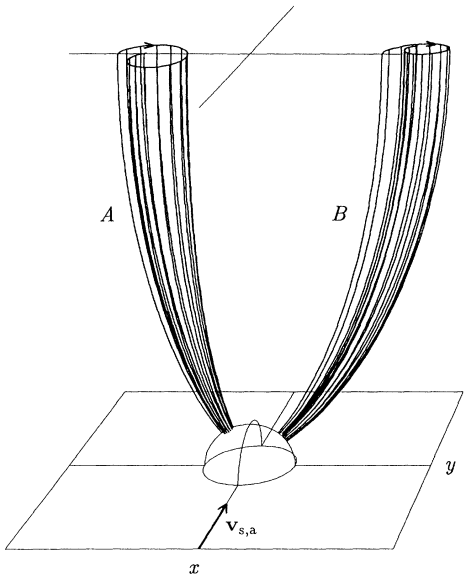

FIG. 14. Motion of a parallel pair on a pinning site under the applied field $v_{s,a} = 0.1$ cm/sec, which is perpendicular to the plane including two initial vortices. The arrows on the top represent the direction of motion.

applied flow field for A and parallel for B. As the applied field increases, vortex B bends more, eventually to be depinned from the pinning site. The consideration finds that the critical depinning velocity $v_{p,2}$ of B is smaller than that of only one vortex trapped on the sphere. The value of $v_{p,2}$ is actually found to be about 0.2 cm/sec by

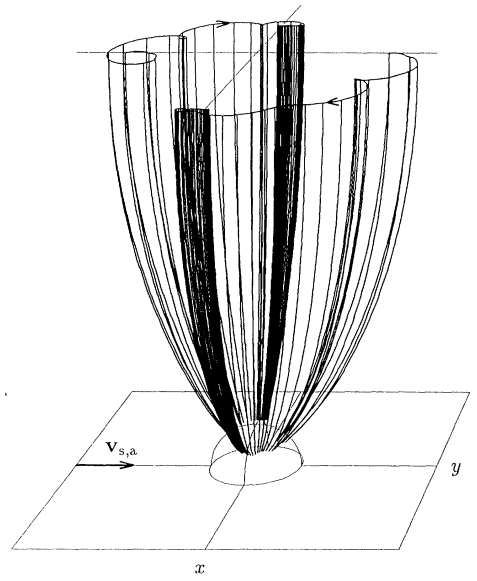

FIG. 15. Motion of a parallel pair on a pinning site under the applied field $v_{s,a} = 0.1$ cm/sec, which is parallel to the plane including two initial vortices. The arrows on the top represent the direction of motion.

numerical calculations; it is smaller than that described in Sec. III. Figure 15 shows another case where the applied field is parallel to the plane including two initial vortices. They rotate around the pinning site to relax to the same equilibrium configuration as Fig. 14. The present critical velocity is about 0.2 cm/sec similarly.

VI. CONCLUSION AND DISCUSSION

This section summarizes the complicated story described in previous sections. First we refer to the motion of two antiparallel vortices. When there is a vortex B near a pinning site with another A, B is attracted into it [Fig. 16(a)]. Then there are two possibilities for B; one is that B is captured by the sphere without interruption [Fig. 16(b)], and the other that B reconnects with A previous to the sphere [Fig. 16(c)]. The former case is followed by two vortices reconnecting just on the sphere [Fig. 16(d)] or at a point apart from it [Fig. 16(e)]. The new vortex C resulting from the reconnection on the sphere goes away because of its local-induced field [Fig. 16(f)]. The reconnection apart from the sphere produces two new vortices D and E [Fig. 16(g)], both of which leave the site [Fig. 16(h)]. On the other hand, two new vortices [Fig. 16(i)] given by the reconnection shown in Fig. 16(c) go away from the site [Fig. 16(j)]. Anyway, a vortex pinned on the pinning site becomes depinned when another antiparallel one approaches, and none are left behind there. These results are not changed qualitatively by an applied superflow field.

The scenario of two parallel vortices is different [Fig. 17(a)]. They never reconnect with each other. The nonlocal field tends to prevent the pinning site from trapping B. Only when B happens to meet the sphere during its rotational motion due to the nonlocal interaction, can the sphere trap it. This is expected to occur often in remnant vortices of superfluid at rest as long as the boundary surfaces are not so specular. Two vortices on the sphere do the characteristic rotation [Fig. 17(b)], relaxing to an equilibrium configuration because of mutual friction [Fig. 17(c)]. Three vortices on the sphere, whose

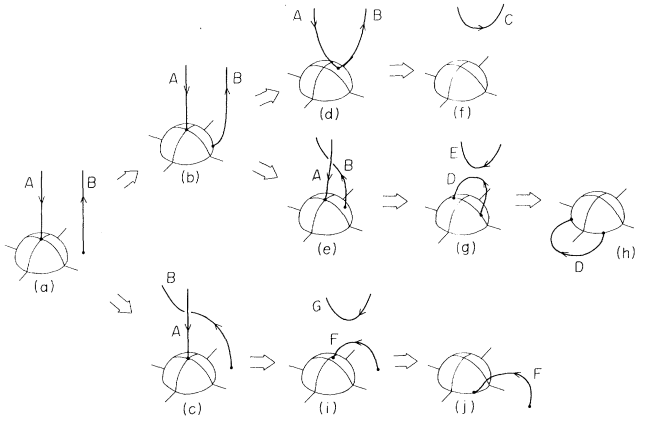

FIG. 16. Summary of motion of an antiparallel pair without an applied field. See the text.

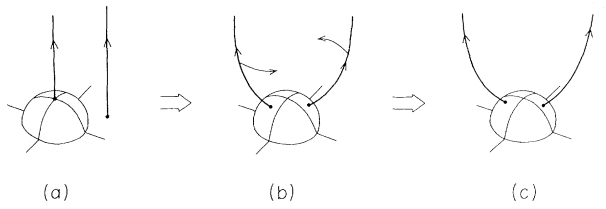

FIG. 17. Summary of motion of a parallel pair without an applied field. See the text.

motion is not calculated, may follow a similar process. A pinning site is believed to have the capacity for capturing parallel vortices; the capacity probably depends on the sphere and channel size. Assuming the vortex to be infinitely thin, the present formulation cannot investigate the capacity.

The dynamics of two parallel vortices is influenced a great deal by an applied superflow field $v_{s,a}$. The previous sections had three kinds of critical velocity. A strong applied flow above $v_{p,1}$, which is the critical depinning velocity of only one vortex trapped on the pinning site, would blow off vortex A. Only the applied flow above v_c can make vortex B reach the pinning site that has already captured A. Furthermore, even once vortex B is trapped, both vortices cannot stay on the site when $v_{s,a}$ is larger than the critical depinning velocity $v_{p,2}$ of the two vortices described in the preceding section. Therefore, only when $v_c < v_{s,a} < v_{p,1}, v_{p,2}$, can the pinning site keep both vortices. Our numerical calculations show, however, that the values of $v_{p,1}$, $v_{p,2}$, and v_c are, respectively, about 0.4, 0.2, and 0.3 cm/sec. Thus a pinning site can hardly keep two parallel vortices together under an applied superflow field. However, since these critical velocities depend on the geometry, we may have the case that satisfies the above condition of $v_{s,a}$.

These results are compared with experiments described in Sec. I. To understand the difference of the observed critical velocity between rough and smooth surfaced rotating channels,[2] Hegde and Glaberson solved the nonlinear equations stating that the net force on a stationary vortex, Magnus force plus friction force, must be zero, when the nonlocal field was neglected. The calculated values of critical heat flux agreed well with their data. Our present results considering the nonlocal field are qualitatively consistent with the experimental results. The rotating channel contains parallel vortices whose density depends on the rotation speed. The smooth surface means less protrusions on it. Thus it happens more often for two vortices to be captured by the same pinning site. It follows that the critical depinning velocity is expected to be smaller than that in a rough surface. The spin-up problem studied by Adams[3] can be understood similarly. They observed responses of smooth and rough surfaced cells to an impulsive torque. The former relaxed faster than the latter, which is compatible with the smaller depinning velocity of the former. Phase slippage can be an important application of our present calculation. The phenomena is believed to depend on the details of aperture geometry, flow direction, and temperature. Whether a vortex is nucleated thermally or quantum mechanically, it moves according to the above scenario. Thus, the comparison with experimental data needs a further calculation for various values of parameters, such as D, b, the channel length, and temperature.

ACKNOWLEDGMENT

The numerical calculation in this work was done by the use of CRAY Y-MP8 at the Institute of Fluid Science, Tohoku University.

[1] R. J. Donnelly, *Quantized Vortices in Helium II* (Cambridge University Press, Cambridge, 1991).
[2] S. G. Hedge and W. I. Glaberson, Phys. Rev. Lett. **45**, 190 (1980).
[3] P. W. Adams, M. Cieplak, and W. I. Glaberson, Phys. Rev. B **32**, 171 (1985).
[4] D. D. Awschalom and K. W. Schwarz, Phys. Rev. Lett. **52**, 49 (1984).
[5] O. Avenel and E. Varoquaux, Phys. Rev. Lett. **55**, 2704 (1985); E. Varoquaux, M. W. Meisel, and O. Avenel, *ibid.* **57**, 2291 (1986); O. Avenel and E. Varoquaux, *ibid.* **60**, 416 (1988).
[6] A. Amar, Y. Sasaki, R. L. Lozes, J. C. Davis, and R. E. Packard, Phys. Rev. Lett. **68**, 2624 (1992).
[7] J. C. Davis, J. Steinhauer, K. Schwab, Yu. M. Mukharsky, A. Amar, Y. Sasaki, and R. E. Packard, Phys. Rev. Lett. **69**, 323 (1992).
[8] G. G. Ihas, O. Avenel, R. Aarts, R. Salmelin, and E. Varoquaux, Phys. Rev. Lett. **69**, 327 (1992).
[9] K. W. Schwarz, Phys. Rev. B **31**, 5782 (1985).
[10] K. W. Schwarz, Phys. Rev. B **38**, 2398 (1988).
[11] K. W. Schwarz, Phys. Rev. Lett. **57**, 1448 (1986).
[12] K. W. Schwarz, Phys. Rev. Lett. **59**, 1167 (1987).
[13] K. W. Schwarz, Phys. Rev. Lett. **64**, 1130 (1990).
[14] M. Tsubota and S. Maekawa, J. Phys. Soc. Jpn. **61**, 2007 (1992).
[15] K. W. Schwarz (unpublished).
[16] W. I. Glaberson and R. J. Donnelly, Phys. Rev. **141**, 208 (1966).